Constraints on the EOS of neutron star matter based on observations

Ngo Quang Thin
Graduate School of Engineering
Gifu University

A thesis submitted for the degree of
Doctor of Engineering
Gifu 2018

This thesis is dedicated to
my family
for their love, endless support and encouragement.

Acknowledgements

I would never have been able to finish my thesis without the guidance of my supervisors, help from friends, and support from my family.

First and foremost, I would like to express my deepest gratitude to my advisor, Prof. Shoji Shinmura, for his excellent guidance, caring, patience, and providing me with an excellent atmosphere for doing research. Without his assistance and dedicated involvement in every step throughout the process, this thesis would have never been accomplished. I would like to thank you very much for your support and understanding over these past three years.

Most importantly, none of this could have happened without my family. To my parents, my sister and my brother-in-law it would be an understatement to say that, as a family, we have experienced some ups and downs in the past three years. Every time I was ready to quit, you did not let me and I am forever grateful. This thesis stands as a testament to your unconditional love and encouragement.

Abstract

Numerous computations of the neutron star equation of state (EOS) have been performed throughout the years. Recent neutron star observations have exhibited and started to assume a critical role in finding the realistic EOS. In this thesis, we analyze mass-radius relations derived from various EOSs with observational data of neutron stars. Furthermore, we adjust EOSs to be consistent with observational data of neutron stars and employ Bayesian statistical analyses to obtain constraints on EOS. Our results demonstrate that EOS needs to be softened at the medium density region (2-4 times of the saturation density) and has a rapid change of stiffness around the energy density $\sim$ 650 MeV/fm^3.

Contents

List of Figures

Chapter 1

Introduction

Neutron star is a star composed of neutrons. In spite of the fact that neutron stars normally have a radius at the order of 10 km, they could have masses of about twice that of the solar. The average density is more than 10^{14} times the density of the sun. Due to its extraordinarily high density of approximately 10^{17} kg/m^3 (the Earth has a density of around 5×10^3 kg/m^3), the surface gravity of the neutron stars is as large as 2×10^{11} times the surface gravity of the earth, and the escape speed reaches $c/3$ (where c is the speed of light). A neutron star is formed as a result of its central core being compressed by a supernova explosion of a giant star. The existence of neutron stars was predicted in 1933, however, it was not discovered until 1967 that rapidly spinning neutron stars, known as pulsars were detected. There are at present over 2,000 neutron stars known in the disk of the Milky Way. Many discussions were made on the structure of neutron star so far, however many mysteries are nonetheless left. Although various equation of state (EOS) representing the structure of neutron stars have been proposed, our knowledge of neutron star structure is still limited. Moreover,in recent years neutron stars which have not been explained by theory were discovered. Therefore, the theory so far need to be reconsidered.

Among neutron star research, EOS of neutron star matter is one of central issues. Because the average densities of typical neutron stars are about two times of the nuclear density ($\approx 3.0 \times 10^{14}$g/cm^3), explanation of EOS of neutron stars is one of fundamental problems in nuclear physics. The EOS determines properties such as the neutron star cooling, maximum mass, the mass-radius relationship, the saturation densities, etc. Establishing a reasonable neutron star matter EOS which can support observed masses and radii of neutron stars is the focal point of researchers thinking. Further, the recent discovery of the heavy neutron stars PSR J1614+2230[9] with mass $M = 1.97 \pm 0.04\ M_\odot$ and PSR J0348+0432[4] with mass $M = 2.01 \pm 0.04\ M_\odot$, has delivered a lot of challenge in this problem. Because most of EOS are too soft

to sustain the neutron star mass 2 $M_\odot$ (even 1.4 $M_\odot$), the stiffer EOS seem to be needed. In addition, the difficulty called *hyperon puzzle*[48] in which the appearance of new degrees of freedom softens EOS and the maximum mass of neutron stars is reduced considerably makes neutron star research more difficult. By constructing the EOS giving the maximum mass of neutron stars larger than 2 $M_\odot$, we can find the solution to the *hyperon puzzle* problem in principle. Many nuclear physicists have been attempted to solve these difficulties such as in frameworks based on the model with quark-meson coupling[23,28,45] and the vector baryon-fmeson coupling model.[51] By stiffing the EOS in high densities, such as the hadron-quark crossover,[27] the universal repulsive three-body force effect,[31,53] the maximum mass can increase up to $\approx 2\ M_\odot$. In high-density region, physical effects such as many-body forces, boson condensations or effects of quark degrees of freedom are proposed and expected to be important.

In particular, the recent studies of neutron star radii are extremely important, because it rejects a large number of EOS. Recent observations of neutron stars have presented evidence that range of possible neutron star radii $= 9.1^{+1.3}_{-1.5}$ km (90%-confidence).[18] The stiff EOS can support a 2 $M_\odot$ neutron star but are not compatible with the small neutron star radii. Because most of the EOSs are compatible with large radii ($\approx$12 km; see Fig. 5.2), it is necessary to adjust the EOS to be consistent with small radii. For this problem, we introduce the phenomenological third order term of baryon density to control the stiffness of EOS and extend the EOS to high densities by assuming a parametric form. The adjustable parameters are fixed utilizing the statistical method developed by Steiner et al. to be consistent with observational data of neutron stars. In this thesis, by comparing mass-radius (M-R) relations derived from various EOSs with observational data, we discuss the properties of the probable EOS. Our aim is to establish realistic constraints on the neutron star matter EOS.

This thesis consists of six chapters, including this introduction. Below is a summary of the major contents of each chapter.

In chapter 2, we start by briefly introducing some basic knowledge of neutron star matter EOS. Then we propose our EOS model to describe neutron star structure. The purpose of this chapter is to provide an overview of our EOS parameters.

Chapter 3 describes the Tolman-Oppenheimer-Volkov equations that are fundamental ingredients to calculate mass-radius of neutron star. From the Einstein equations, we formulate and derive the Tolman-Oppenheimer-Volkov equations that describe neutron star structure.

Chapter 4 is subdivided into two parts. The first provides the Bayesian analysis and the second discusses observational data. While not all of the uncertainties

involved in constraining the mass and radii of neutron stars are under control, it is important to quantify the constraints on the EOS which are implied by the observations.

Chapter 5 concerns constraints on the EOS and saturation properties. In this chapter, we review existing literature in saturation properties and discuss the properties of appropriate EOS obtained from this work.

Finally, chapter 6 is devoted to give the summary of this work and also to propose some future plan.

Chapter 2

Equation of State

A description of neutron star structure is obtained by constructing the equation of state (EOS). In physics, an EOS is an equation relating state variables pressure and energy density (or baryon density) which describes the state of matter. In this thesis, we divide EOS to the three regions as illustrated in Fig. 2.1. The first region is the crust of neutron stars. The second region is the theoretical EOS region defined by the baryon densities from $\rho_0/2$ to $n\rho_0$, where n is a variable and $\rho_0 = 0.17$ fm^{-3} is the saturation density. The third region is that with densities higher than n times of the saturation density. This region is described by the EOS satisfying the causality condition ($dp/d\epsilon < 1$).

2.1 Crust EOS Region

The first region is the crust of neutron stars. The mass of neutron star crustconstitutes only 1% of the neutron star mass and its thickness is typically less than onetenth of the star radius. The crust of neutron stars with densities ranging from 0.0 to 0.5 times of nuclear density extends down to about 1 kilometer below the surface. To construct crust EOS of neutron star we need knowledge in many different research fields such as nuclear reactions, physical kinetics, the nuclear many-body problem, hydrodynamics, the physics of liquid crystals, superfluidity, etc. The research of neutron star crust EOS is numerous and represents very different theoretical challenges. Most of the research contributes to description of neutron star crust EOS in many aspects. Because the EOS of the crust of a neutron star can be well-described by a model formulated in the classical paper of Baym, Pethick, and Sutherland (BPS),[7] in this region, we use BPS EOS and its extrapolation up to the transition baryon density up to the transition baryon density $\rho_{crust} = \rho_0/2$, where $\rho_0 = 0.17$ fm^{-3} is the nuclear

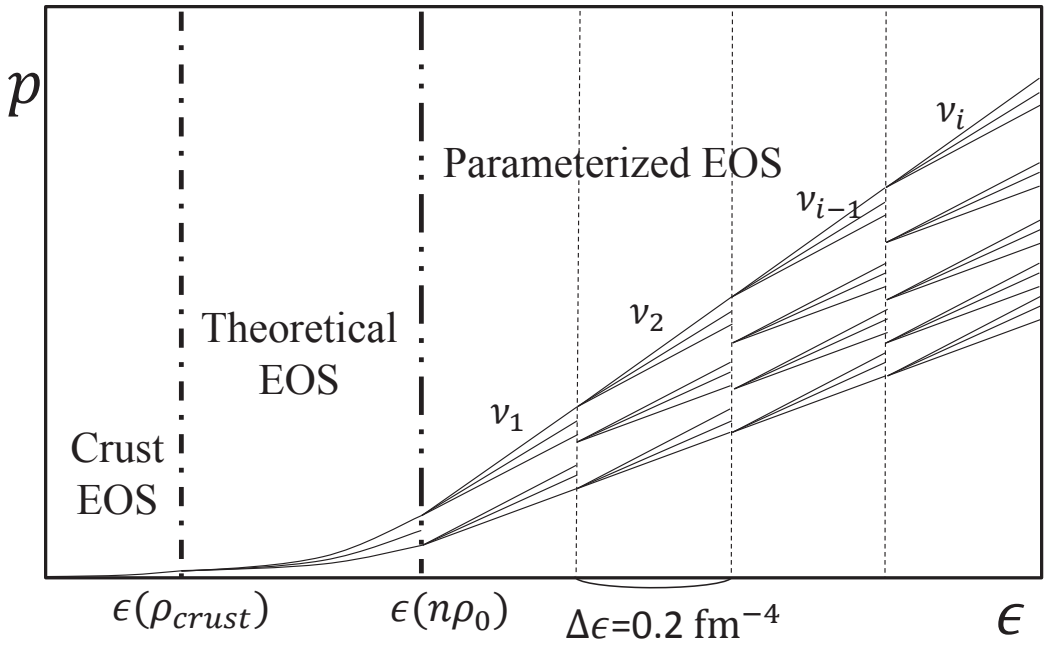

Figure 2.1: EOS structure. Pressure p as the function of energy density ϵ. In high-density region, we use parameterized EOS which is the general piece-wise linear function. We take $\rho_{crust} = \rho_0/2$, $2 \leq n \leq 5$ and $0 < \nu_{1,\ldots,i} \leq 1$.

saturation baryon density. Table C.1 (Appendix C)[15] shows the EOS of neutron star matter at subsaturation densities is due to Baym, Pethick and Sutherland.[7]

2.2 Theoretical EOS Region

The second region is the theoretical EOS region defined by the baryon densities from $\rho_0/2$ to $n\rho_0$, where n is a variable. This region that is the main region of the present thesis, represents very different theoretical challenges. Although a large number of different EOSs has been supposed, the EOS for this region is still not well-known. From a theoretical perspective, they can generally be separated into three groups. The first includes EOSs based on phenomenological nuclear interactions. Two-nucleon (NN) interactions were formulated to fit NN scattering experiments at low energies. Since two-nucleon interactions by themselves cannot completely explain the properties of nuclear matter, three-nucleon (3N) interactions were introduced. Many-body prob-

lems based on NN and 3N interactions are still very difficult to solve owing to strong forces at relatively small distances, which lead to expanding higher order wave functions. The second group incorporates EOSs based on effective field theory (EFT) approaches. The development of chiral EFT has provided a framework for a systematic expansion for nuclear forces at low momentum, where nucleons interact by pion exchange and short-range interactions. The advancements of EFT are that it utilizes less parameters and has high predictive power. In recent years, the chiral EFT has become more and more popular. The third group of EOSs is characterized by their inclusion of softening components at high densities, such as hyperons[13] and boson condensates (kaon condensates[16]), or the assumption of a single first-order phase transition between nuclear and quark matter.

In this region, we assume the energy density given by

$$\begin{aligned} \epsilon &= \epsilon_{theo}(\rho) + \epsilon_3\rho^3 \quad \text{for} \quad \rho_{crust} < \rho < n\rho_0 \\ p &= p_{theo} + 2\epsilon_3\rho^3, \end{aligned} \tag{2.1}$$

where ϵ and ρ are the energy density and the baryon density, respectively. The ϵ_{theo} and p_{theo} are determined from various EOS models and the ϵ_3-term is introduced as a phenomenological third order term of baryon density. The ϵ_3-term does not mean directly the three-body force effect. It is well known that for a given neutron star mass, the neutron star radius depends on how stiff or soft the EOS is. A. W. Steiner et al. estimated that the radius of a neutron star with mass 1.4 $M_\odot$ is between 10.4 and 12.9 km.[43] Because neutron star radii are mainly decided by theoretical EOS in the second region, the ϵ_3-term plays a role in controling neutron star radii.[46] The ϵ_{theo} is taken from many different EOS models. Among them, we choose typical EOSs and use them as the theoretical EOS in the second region based on their saturation property.

2.3 Parameterized EOS Region

The third region is that with densities higher than n times of the saturation density. This is the neutron star core region. This region is described by the EOS satisfying the causality condition ($dp/d\epsilon < 1$). However, the inner structure of neutron stars is is a huge challenge to theorists due to the theoretical and observational uncertainties. Theoretically, the inner core of neutron stars with very high density is expected to be composed of various exotic particles, such as pions, kaons, hyperons[15] and strange quark states[37,50]. However, EOS of dense matter beyond the nuclear density are still

quite uncertain in particle and nuclear physics. Because of these uncertainties, EOS of neutron star core region is not well-known. But when calculating M-R relation of neutron stars, we need EOS to solve the system of TOV equations. Therefore in neutron star core region, we assume the pressure $p(\epsilon)$ as a parameterized piecewise linear function of the energy density ϵ given by

$$p(\epsilon) = \begin{cases} p_{i-1} + \nu_i(\epsilon - \epsilon_{i-1}) & \text{for } \epsilon_{i-1} \leq \epsilon \leq \epsilon_i (i = 1 \sim (N-1)) \\ p_{N-1} + \nu_N(\epsilon - \epsilon_{N-1}) & \text{for } \epsilon_{N-1} \leq \epsilon, \end{cases} \tag{2.2}$$

with

$$\begin{aligned} \epsilon_i &= \epsilon_0 + i\Delta\epsilon (i = 1 \sim (N-1)), \\ p_i &= p_{i-1} + \nu_i \Delta\epsilon (i = 1 \sim (N-1)), \end{aligned} \tag{2.3}$$

where ν_i is slope parameters.

Here we use totally eight parameters $n, \epsilon_3, \nu_{1,\ldots,4}$ to construct neutron star EOS. The six linear functions ($N = 6$) with slopes $\nu_{1,\ldots,6}$ and the $\Delta\epsilon$ parameter make it possible to vary the stiffness of EOS at high-density region. Note that we parameterize the high-density EOS as a function of the energy density ϵ. We choose the $\Delta\epsilon = 0.2$ fm^{-4} and the transition baryon density $n\rho_0 = (2.0\text{-}5.0)\ \rho_0$. The p_0 is determined by continuity of $p(\epsilon)$ at the transition density $\epsilon_0 = \epsilon(n\rho_0)$. We vary the slope parameters over the ranges $\nu_{i-1} \leq \nu_i < 1$ (the causality condition). In numerical calculations, we confirmed that $N = 6$ and $\Delta\epsilon = 0.2$ fm^{-4} is suitable values to ensure that EOS at high-density region could be parameterized reasonably well and results are not changed significantly even if additional linear functions are introduced. By extending EOS to higher densities in this way, we hopefully achieve constraints on the EOS not only in the secon region but also the third region.

Chapter 3

Tolman-Oppenheimer-Volkov Equation

3.1 Introduction

The Tolman-Oppenheimer-Volkoff (TOV) equations[32,47] derived from the Einstein equations play an important role in determining neutron star mass-radius relation. These equations constrains the structure of neutron stars. For a given EOS, masses and radii of neutron stars can be determined as functions of central pressure (or central energy density) by solving the TOV equation.

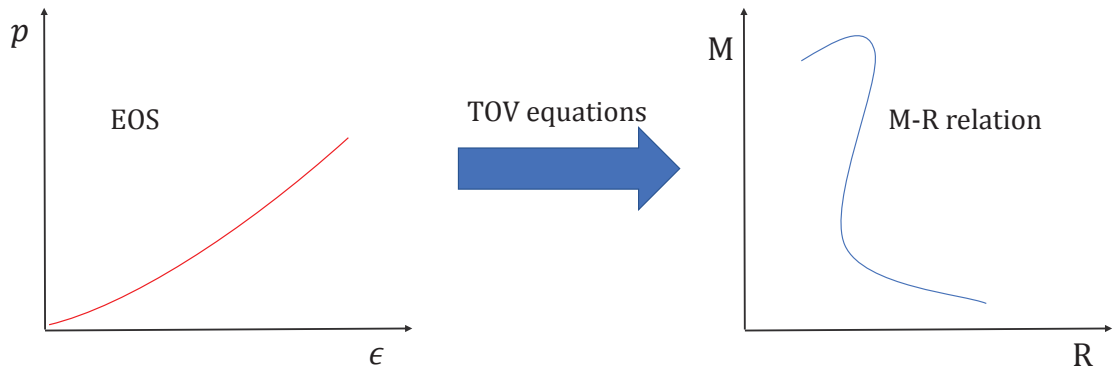

Figure 3.1: Masses and radii of neutron stars can be determined by solving the TOV equation using EOS. The EOS has a one-to-one correspondence to the mass-radius curve.

3.2 The Tolman-Oppenheimer-Volkoff Equation

Start with the Einstein equation,

$$G^{\mu\nu} = \frac{8\pi G}{c^4} T^{\mu\nu} \tag{3.1}$$

here $G^{\mu\nu}$ is the Einstein tensor, describing the curvature of spacetime and $T^{\mu\nu}$ is the stress energy tensor, describing matter/energy sources of spacetime curvature. We also have

$$T^{\mu\nu} = -pg^{\mu\nu} + (p+\epsilon)u^{\mu}u^{\nu} \tag{3.2}$$

Where, ϵ is the energy density, p is the pressure, u^{μ} is the four-velocity, and $g^{\mu\nu}$ is the four-metric which we use to measure distances in spacetime ($ds^2 = g_{\mu\nu}dx^{\mu}dx^{\nu}$).

It is well known that Schwarzschild metric gives line element ds^2 as the following formula:

$$ds^2 = -e^{2\phi(r)}c^2dt^2 + \left(1 - \frac{2Gm(r)}{rc^2}\right)^{-1} dr^2 + r^2 d\Omega^2 \tag{3.3}$$

Here, $m(r)$ is the mass inside radius r, $e^{\phi(r)}$ is the lapse function and $\phi(r)$ will be called the metric potential.

Assuming zero space velocity, spherical symmetry and using eq. (3.3), the stress energy tensor of eq. (3.2), we can solve and reformulate eq. (3.1). Tolman, Oppenheimer, and Volkoff worked this out and arrived a system of ordinary differential equations, the so-called TOV equations:[32,47]

$$\frac{dp}{dr} = -\frac{G}{r^2}\left[\epsilon + \frac{p}{c^2}\right]\left[m + \frac{4\pi r^3 p}{c^2}\right]\left[1 - \frac{2Gm}{rc^2}\right]^{-1}, \tag{3.4}$$

$$\frac{dm}{dr} = 4\pi r^2 \epsilon \tag{3.5}$$

Here G is gravitational constant. In the case of neutron star, m is mass, r is radius of neutron star and $m(r)$ is the mass inside radius r. By set of boundary conditions and using EOS that provides a relationship between energy density and pressure we can solve these equations by numerical integration.

The TOV equations presents hydrostatic equilibrium, i.e. there must be a balance between the pressure and gravity. A stable star must be satisfied this requirement. When we set $G = c = 1$, eq. (3.4) and (3.5) become

$$\frac{dp}{dr} = -(\epsilon + p)\frac{m + 4\pi r^3 p}{r(r-2m)}, \tag{3.6}$$

$$\frac{dm}{dr} = 4\pi r^2 \epsilon \tag{3.7}$$

This is a system of 2 ordinary differential equations with the EOS relating pressure p and energy density ϵ. We can be solved by integrating from $r = 0$ with starting values

$$\epsilon(r = 0) = \epsilon_c,\ p(r = 0) = p_c,\ m(r = 0) = 0, \tag{3.8}$$

where ϵ_c is central energy density and p_c is central pressure. And

$$p(R) = 0,\ m(R) = M, \tag{3.9}$$

where R is neutron star radius and M is neutron star total mass. Our aim is to obtain the mass of the neutron star $M(\epsilon(0)) \equiv M(\epsilon_c)$ as a function of the central energy density and the radius of the neutron star $R(\epsilon(0)) \equiv R(\epsilon_c)$ as a function of the central energy density. This integration yields the pressure profile $P(r)$, and the corresponding energy density profile $\epsilon(r)$ for given central energy density. For the given EOS, there is a unique relationship between the mass and central density. Figure 3.1 shows relationship between EOS, TOV equations and M-R relation.

Chapter 4

Application of Statistical Method to Constraints on the EOS

Because of the lack of observations and experimental data, at present constraining on the neutron star's behaviour and mass-radius relation is still very difficult. Over the past many years a large of sophisticated models have been developed and there have been significant recent works in measuring the radii of neutron stars. Statistical method which were used to bring out the most probable values of mass and radii of neutron stars is one of those works. More information becomes available to allow us to make more realistic constraints. In this thesis, we employ the Bayesian statistical method proposed by Steiner et al.[44] to build up constraints on the M–R relation and the EOS of NS matter. Additionally, using more observational sources enables us to put more reasonable constraints on the EOS of NS matter. Below sections will give a brief introduction of Bayesian framework and the observational data.

4.1 Bayesian Analysis

Let's start with Bayes theorem

$$P(\mathcal{M}|D) = \frac{P(D|\mathcal{M})P(\mathcal{M})}{P(D)}. \tag{4.1}$$

where $P(\mathcal{M})$ is the prior probability of the model $\mathcal{M}$ without any information from the data D, $P(D)$ is the prior probability of the data D, $P(D|\mathcal{M})$ is the conditional probability of the data D given the model $\mathcal{M}$ and $P(\mathcal{M}|D)$ is the conditional probability of the model $\mathcal{M}$ given the data D.

For the select models $\mathcal{M}_i$ which satisfy $\sum_i P(\mathcal{M}_i) = 1$, the eq. (4.1) can be rewritten by

$$P(\mathcal{M}_i|D) = \frac{P(D|\mathcal{M}_i)P(\mathcal{M}_i)}{\sum_i P(D|\mathcal{M}_i)P(\mathcal{M}_i)}. \tag{4.2}$$

For our problem, the model space consists of the EOS parameters, $\{p_i(i = 1, ..., 8)\} = \{n, \epsilon_3, \nu_1, \nu_2, \nu_3, \nu_4, \nu_5, \nu_6\}$ and the masses of neutron stars, $\{M_l(l = 1, ..., 23)\}$. Constructing the EOS by using these parameters, $\{p_i\}$, and solving the TOV equations, a radius $\{R_l\}$ for each of the neutron star masses $\{M_l\}$ is obtained. Because if we assume that the model space consists of only six EOS parameters, we cannot determine uniquely the mass and radius of neutron stars, $\{M_l\}$ parameters but should be included in the data D. Therefore, model parameter, for example, the central pressure p_c to determine uniquely the mass and radius for each neutron star needs to be added. In this treatment, p_c for each l is a function of $\{M_l\}$ and the eight EOS parameters. Therefore, $\{\mathcal{M}$(eight EOS parameters, p_c for $l = 1, ..., 23)\}$ is equivalent to $\{\mathcal{M}$(six EOS parameters, $M_1, ..., M_{23})\}$. On the other hand, p_c depends strongly on the EOS used and its lower and upper bounds are unclear. Therefore, p_c for $l = 1, ..., 23$ are unsuitable as model parameters. This is the reason why we choose to treat $\{M_l\}$ as model parameters. Substituting in the eq. (4.2), we have

$$\begin{aligned} P[\mathcal{M}(\{p_i\}, \{M_l\})|D] &= P[D|\mathcal{M}(\{p_i\}, \{M_l\})] \\ &\times P[\mathcal{M}(\{p_i\}, \{M_l\})] \left[\int P[D|\mathcal{M}]P[\mathcal{M}]d^N\mathcal{M}\right]^{-1}, \end{aligned} \tag{4.3}$$

where $N = N_p + N_M = 8 + 23 = 31$ is the dimension of our model space, where N_p the total number of EOS parameters and N_M is the total number of neutron stars in our data set.

Next step, $P(D|\mathcal{M})$ is proportional to the product over the probability distributions D_l is assumed. The D_l is evaluated at the masses which are determined in the model and evaluated at the radii which are determined from the model $\mathcal{M}$, i.e.,

$$P[D|\mathcal{M}(\{p_i\}, \{M_l\})] \propto \prod_{l=1,...,23} D_l(M, R)|_{M=M_l, R=R(M_l)}. \tag{4.4}$$

More specifically, eq. (4.3) can be rewritten by

$$\begin{aligned} P[\mathcal{M}(\{p_i\}, \{M_l\})|D](\{p_i\}) &\propto \int P[D|\mathcal{M}(\{p_i\}, \{M_l\})]dM_1...dM_{23} \\ &\propto \int \prod_{l=1,...,23} D_l(M, R)|_{M=M_l, R=R(M_l)}dM_l, \end{aligned} \tag{4.5}$$

where the prior probability $P(\mathcal{M})$ is uniform under the several conditions for model parameters: $2 < n < 5$, $0 < \nu_i \leq \nu_{i+1} < 1$, and supporting 2 $M_\odot$. As the data D_l we use the probability distributions D_l $(l = 1, ..., 23)$ derived from neutron star observations listed in Table 4.2. In this work, all of the probability distributions

$D_l(M, R)$ of neutron stars has probability inside of the ranges, $M_{low} < M < M_{high}$ and $R_{low} < R < R_{high}$. We choose $M_{low} = 0.8\ M_\odot$, M_{high} =2.5 $M_\odot$, $R_{low} = 5$ km and $R_{high} = 18$ km. Radii of observed neutron stars used in this work are shown in Table 4.1.

Name	Radius (group 1)	Radius (group 2)	ΔR (km)
4U 1608-52	9.3 ± 1.0[19]	9.80 ± 1.8	+0.50
EXO 1745-248	9.0[34]	10.5 ± 1.6	+1.50
4U 1820-30	9.11 ± 0.4[20]	11.1 ± 1.8	+2.00
X7 in 47 Tuc	$14.5^{+1.8}_{-1.6}$[21]	$11.1^{+0.8}_{-0.7}$	−3.40
M13	9.77[49]	10.9 ± 2.3	+1.13
ω Cen	11.66[49]	9.40 ± 1.8	−2.26
NGC2808	9.1[49]		
U24 in NGC6397	$8.9^{+0.9}_{-0.6}$[17]	9.20 ± 1.8	+0.30
KS1731-260	9.4 ± 0.3[33]	10.0 ± 2.2	+0.60
SAX J1748		11.7 ± 1.7	
4U 1724		12.2 ± 1.4	
M28		8.50 ± 1.3	
M30		11.6 ± 2.1	
NGC 6304		10.7 ± 3.1	
X5		$9.60^{+0.9}_{-1.1}$	
Average	10.08	10.45	0.36

Table 4.1: Radii of observed neutron stars. ΔR shows the radius difference between group 1 and group 2.

4.2 Observed Masses and Radii of Neutron Stars

The first observational data of neutron star was discovered in 1967. There are at present over 2,000 neutron stars known in the disk of the Milky Way but only about 60 neutron star masses have been determined so far. Because of their unusual characteristics, detecting neutron stars requires different technique than those used to detect normal stars. Neutron stars have two essential attributes that researchers can identify. The first is neutron star's gravitational force in which neutron stars can be detected by how their gravity affects to objects around them. The second is the detection of pulsars which are the highly magnetized, rotating neutron star or white dwarf. Because of fast rotation that created by the gravitational pressure, pulsars emit electromagnetic radiation and this radiation can be observed.

The available neutron star observations with masses and radii simultaneously measured allow us to research neutron star EOS more comprehensively. Using the currently available data with somewhat large uncertainties on estimated masses and radii, we can make intial constraints on the EOS of neutron star. The observational data used here is divided into 2 groups. The first is the 9 neutron stars which derived form original sources. The second is the 14 neutron stars which obtained from Feryal Özel et al. work.[35] We must note that for the same observational source there are different assumptions and techniques used to calculate neutron star massed and radii. Therefore, there are multiple probability distributions for the same observational source. In this work, we do not plan to discuss which technique is preeminent. We respect and employ all of the probability distributions. That is, we have used 23 probability distributions obtained from 15 observational sources (see Table 4.1).

4.2.1 Group 1

The first group consists of the 9 neutron stars which derived from original sources. Their information of masses and radii was obtained from astrophysical observations of X-ray bursts and thermal emissions from quiescent low-mass X-ray binaries (LMXBs). When neutron stars pull material away from companion stars they can become much brighter. Using observation of X-rays at different wavelengths, combined with theoretical models of neutron star atmospheres, we can estimate the relationship between the radius and mass of the neutron stars. This work has been performed by Heinke,[21] by Natalie Webb and Didier Barret,[49] and by Sebastien Guillot.[17] All of these observations were done for neutron star binaries in globular clusters. Because of thermonuclear explosions on surfaces, the atmosphere of neutron stars expands. If observers catch one of these bursts, they can calculate its surface area based on the cooling process. After that, when this calculation is combined with independent estimate of the distance to the neutron star, the mass and radius of this star can be estimated. Feryal Özel and Tolga Guver have applied this technique in their papers.[19,20,33,34] The papers referred above provide information about the neutron star M-R relation and we use this information to construct probability distributions D_l.

In detail, the probability distributions for 4U 1608-52 and 4U 1820-30 are described as the Gaussian distribution

$$D_l(M,R) = A_l \exp\left(-\frac{1}{2}\frac{(M-M_c)^2}{\sigma_M^2} - \frac{1}{2}\frac{(R-R_c)^2}{\sigma_R^2}\right), \tag{4.6}$$

with the values given in Table 4.2. For EXO 1745-248, we use

Name	M_c	σ_M	R_c	σ_R
4U 1608-52	1.74	0.14	9.3	1.0
4U 1820-30	1.58	0.06	9.1	0.4

Table 4.2: Parameters in the probability distributions of 4U 1608-52 and 4U 1820-30.

$$D_2(M,R) = A_2\Bigg[a_1 \exp\left(-\frac{1}{2}\frac{(M-M_{c_1})^2}{\sigma_{M_1}^2} - \frac{1}{2}\frac{(R-R_{c_1})^2}{\sigma_{R_1}^2}\right) + a_2 \exp\left(-\frac{1}{2}\frac{(M-M_{c_2})^2}{\sigma_{M_1}^2} - \frac{1}{2}\frac{(R-R_{c_2})^2}{\sigma_{R_2}^2}\right)\Bigg], \tag{4.7}$$

where the values of parameters are given in Table 4.3.

Name	a_1	a_2	M_{c_1}	M_{c_2}	σ_{M_1}	σ_{M_2}	R_{c_1}	R_{c_2}	σ_{R_1}	σ_{R_2}
EXO 1745-248	0.8	0.2	1.7	1.4	9	11	0.15	0.15	0.5	0.5

Table 4.3: Parameters in the probability distributions of EXO 1745-248.

Values of A_l in eqs. (4.6) and (4.7) are determined to normalize probability densities D_l. For six other neutron stars, based on contour figures given in original papers,[21,33] we estimated probability distributions showed in Figs. 4.1, 4.2 and 4.3. Our probability distributions are similar to these given by A. W. Steiner et al.[44] but not the same.

4.2.2 Group 2

The second group is the 14 neutron stars which obtained from Feryal Özel et al. work.[35] A number of methods have been developed that may provide new information on neutron star masses, radii, EOS. Because of small size, it is very difficult to observe neutron stars directly and measure their radius. In the past few years, using the statistical methods with modern X-ray instruments, several mass-radius measurements of neutron stars were estimated by Feryal Özel et al. The probability distributions were derived from the observation data with 2-sigma uncertainties by analysing neutron star thermonuclear bursts and quiescence. They are shown in the Fig. 4.4–4.7 below. The databases can be found on $http://xtreme.as.arizona.edu/NeutronStars/$, home page of the Xtreme Astrophysics Group at the University of Arizona. In previous paper,[46] probability distributions of only group 1 were used. Because the more observation data used, the stronger constraints will be made, in this work, 14 new probability distributions of NSs[35] are added.

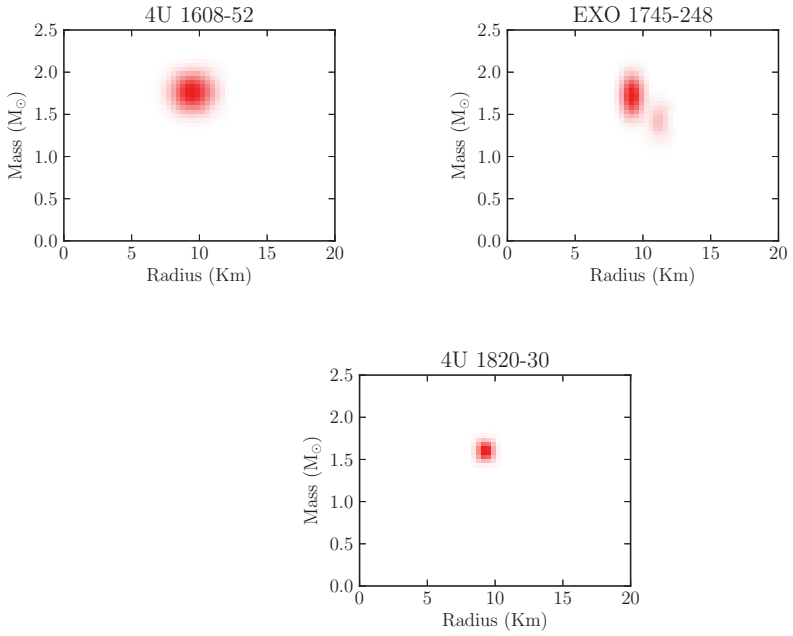

Figure 4.1: Probability distributions D_l described as Gaussian distributions for 4U 1608-52,[19] 4U 1820-30[34] and EXO 1745-248.[20] All distributions are normalized.

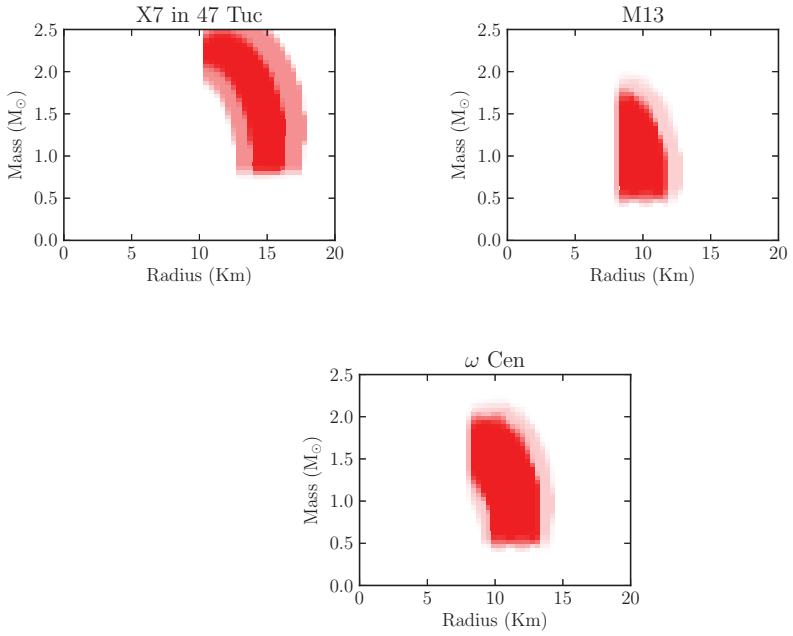

Figure 4.2: Probability distributions D_l for X7 in 47 Tuc,[21] M13, ω Cen.[49] All distributions are normalized.

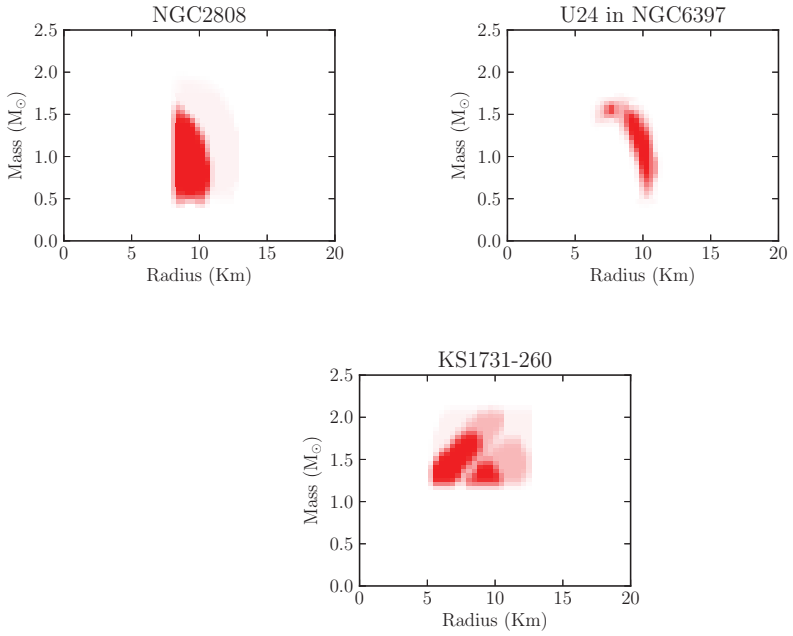

Figure 4.3: Probability distributions D_l for NGC2808,[49] U24 in NGC6397,[17] KS1731-260.[33] All distributions are normalized.

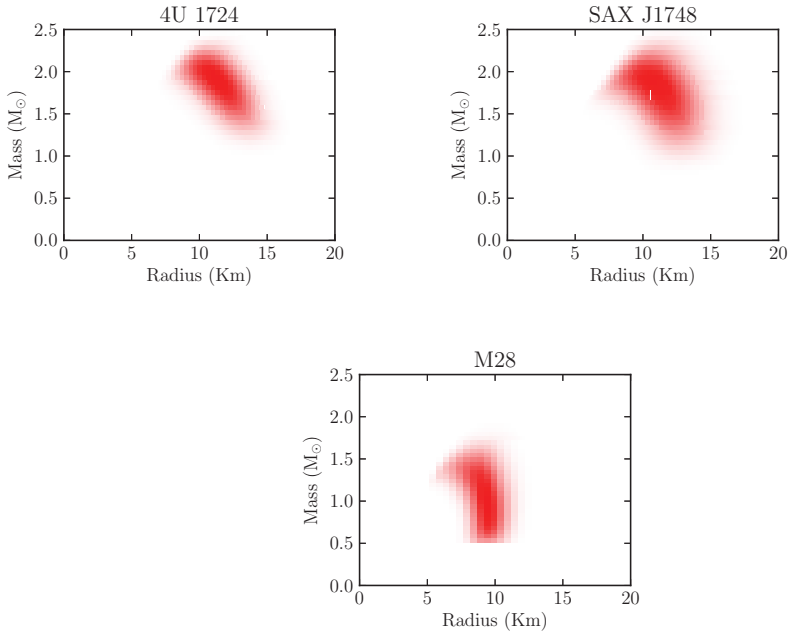

Figure 4.4: Probability distributions D_l for 4U 1724, SAX J1748, M28. All distributions are normalized.

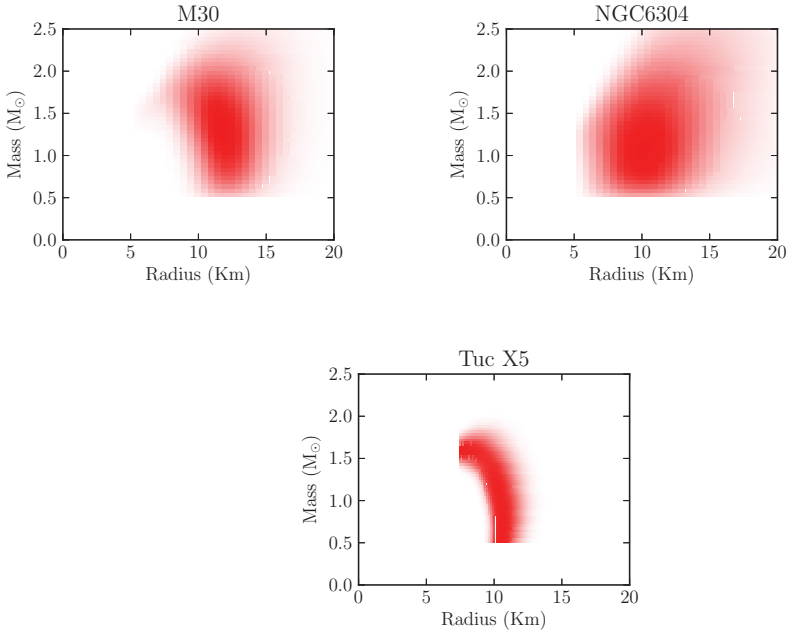

Figure 4.5: Probability distributions D_l for M30, NGC6304, Tuc X5. All distributions are normalized.

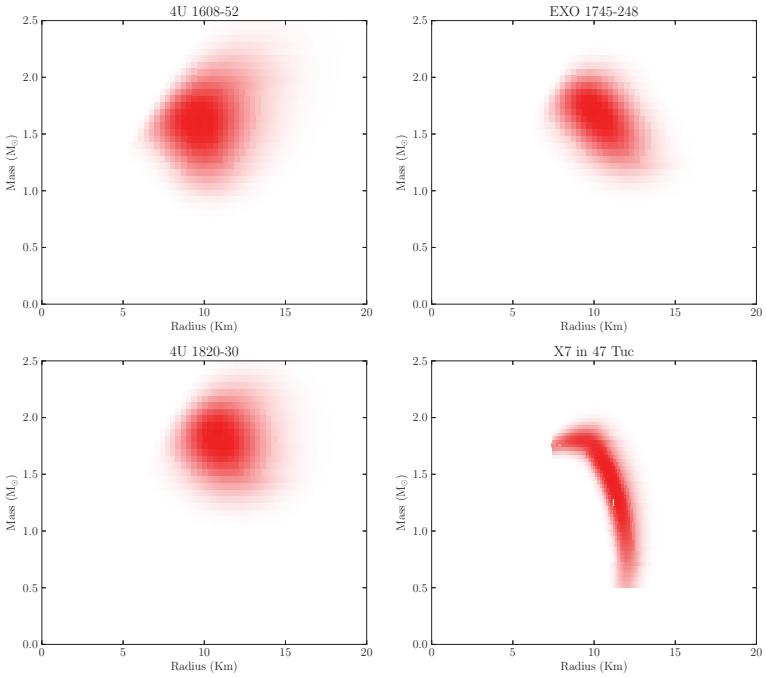

Figure 4.6: Probability distributions D_l for 4U 1608-52, EXO 1745-278, 4U 1820-30, X7 in 47 Tuc. All distributions are normalized.

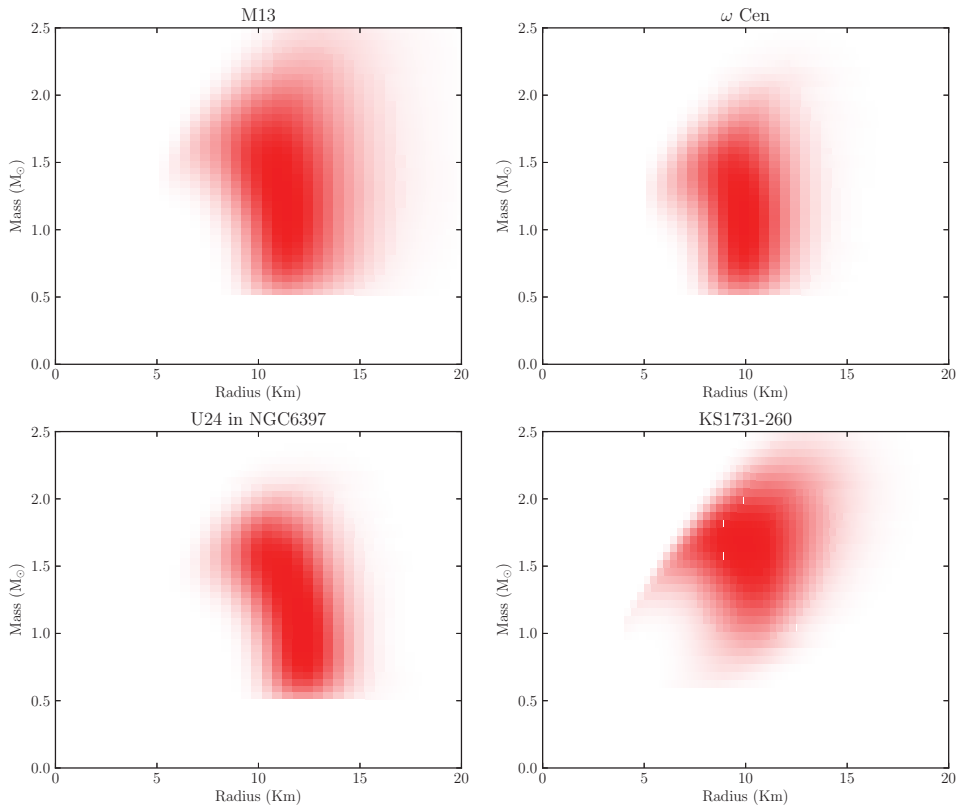

Figure 4.7: Probability distributions D_l for M13, ω Cen, U24 in NGC6397, KS1731-260. All distributions are normalized.

Chapter 5

Results and Discussions

We have employed the Bayesian statistical method proposed by Steiner et al.[44] to make constraints on the M-R relation and the EOS of neutron star matter. Moreover, utilizing more observational sources allows us to place more realistic constraints on the EOS of neutron star matter. By comparing the M-R relation derived by solving the Tolman-Oppenheimer-Volkoff[32,47] equation and the observed data, we discuss the properties of probable EOS.

5.1 Saturation Properties

Saturation properties play an important role in nuclear matter research. The saturation baryon density (ρ_s), the binding energy (B), the symmetry energy (S_v) and its derivative (L) are defined by

$$-B = E(\rho_0, 1/2), \quad S_v = \frac{1}{8}\frac{\partial^2 E}{\partial x^2}\bigg|_{\rho=\rho_0, x=1/2}, \quad L = \frac{3\rho_0}{8}\frac{\partial^3 E}{\partial \rho \partial x^2}\bigg|_{\rho=\rho_0, x=1/2} \tag{5.1}$$

with

$$E(\rho, x) = \frac{\epsilon(\rho, x)}{\rho} - m_n + (m_n - m_p)x, \tag{5.2}$$

where $x = \rho_p/\rho$ denotes the proton fraction ($x = 1/2$ corresponds to symmetric nuclear matter) and m_p (m_n) is the proton (neutron) rest mass. To determine adequate theoretical EOS of neutron star matter, we must calculate the symmetry energy S_v and the L parameter (the slope of the neutron matter energy density) from the neutron star matter EOS. We assume that neutron star matter at normal density consists of neutrons with some electron and proton mixing and obtain[25]

$$\epsilon_\beta(n_s) = n_s\left(E(n_s, x = 1/2) + S_v(1 - 2x)^2 + m_B\right) + \epsilon_e(n_s x), \tag{5.3}$$

$$p_\beta(n_s) = \frac{L}{3} n_s \left(1 - x(4 - 12\frac{S_v}{L})\right) - \epsilon_e(n_s x). \tag{5.4}$$

From these equations and the β-stability condition,

$$\frac{\partial \epsilon_\beta(n = n_s)}{\partial x} = 0 \tag{5.5}$$

and

$$E(n_s, x = 1/2) = -15.7 \text{ MeV}/A \quad \text{for} \quad n_s = 0.17 \text{ fm}^{-3}, \tag{5.6}$$

we determine S_v, L, and x (the proton fraction) for given $\epsilon_\beta(n_s)$ and $p_\beta(n_s)$. In Fig. 5.1, we show S_v and L for various neutron star EOS. We find four groups, A–D, as listed in Table 5.1. Among them, we select typical EOSs from each of the groups and use them as the theoretical EOSs in the second region.

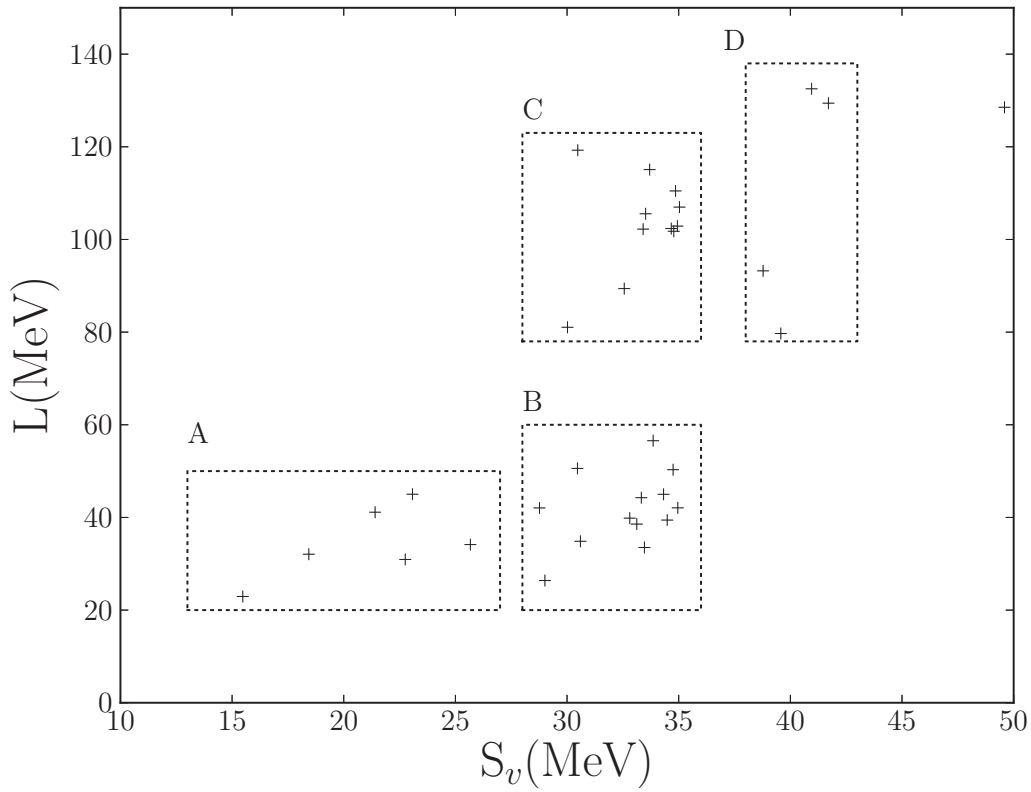

Figure 5.1: Symmetry energy S_v and L parameter at saturation density. Based on S_v and L values we divide EOSs into four groups (A–D). EOS names are listed in Table 5.2.

The EOSs employed in the theoretical EOS region are summarized in Table 5.2. From group A, we select the EOS labeled as AP1 (the AV18 potential).[2] From group

Group	EOS name
A	AP1-4,[2] ALF2,[3] WFF3[52]
B	ALF1,[3]ALF3-4,[3] BBB2,[6] BSK19-21,[39] FPS,[12]ENG,[11] MPA1,[29] WFF1-2,[52] SLY[10]
C	H1-7,[24] MS1,[30] MS1b,[30] PAL6,[40] PCL2[41]
D	BGN1H1,[5] BPAL12,[54] GS2,[42] MS2[30]

Table 5.1: Summation of the EOS model's property.

B, we take the nuclear-quark matter EOS ALF1,[3] the many-body theory EOS BBB2[6] with the AV14 potential plus three-body forces, and the EOS BSK19,[39] which is based on nuclear energy density functional theory with generalized Skyrme effective forces. The Dirac–Brueckner–Hartree–Fock ENG,[11] MPA1,[29] and the variational method FPS[12] are also considered. Finally, we discuss the EOS SLY,[10] which is based on the Skyrme-type effective NN interaction, and The EOS WFF1 obtained in variational calculations of Wiringa et al.[52] The EOS labeled as PAL6 from the phenomenological nonrelativistic potential model of Prakash et al.[40] is taken from group C. The incompressibility of PAL6 has $K = 120$ MeV. From group D, we choose two types of EOS. The first is the EOS BGN1H1,[5] which is obtained in the framework of the Brueckner–Bethe–Goldstone (BBG) theory by assuming a realistic NN potential and a model of the 3N interaction. The second is the EOS BPAL12,[54] which is a soft EOS characterized by a nuclear incompressibility $K = 120$ MeV; it is a nonrelativistic model for the EOS that has been developed to describe hot asymmetric nuclear matter.

Name	Reference	Approach	Composition
ALF1	[3]	Nuclear+quark matter	quark (u, d, s)
AP1	[2]	Variational method	np
BBB2	[6]	BBG theory	$npe\mu$
BGN1H1	[5]	BBG theory	$npe\Lambda\Xi\mu$
BPAL12	[54]	BBG theory	$npe\mu$
BSK19	[39]	Nuclear energy-density functional theory	$npe\mu$
ENG	[11]	Dirac–Brueckner–Hartree–Fock	np
FPS	[12]	Variational method	$npe\mu$
MPA1	[29]	Dirac–Brueckner–Hartree–Fock	np
PAL6	[40]	Schematic potential	np
SLY	[10]	Skyrme-type effective interaction	$npe\mu$
WFF1	[52]	Variational method	np

Table 5.2: Equations of State

5.2 EOS Constraints

In particular, the recent discovery of the two neutron stars PSR J1614+2230[9] and PSR J0348+0432[4] is extremely important, because their properties allow us to reject a large number of EOSs. Furthermore, the radii of several neutron stars have been measured from modeling X-ray bursts and quiescent low-mass X-ray binaries. Recent observations of neutron stars have presented evidence that the range of possible neutron star radii is $9.1^{+1.3}_{-1.5}$ km (at 90% confidence).[18] Because most of the EOSs are compatible with large radii $\approx$ 12 km, it makes the problem more challenging than ever. For that reason revisiting the EOS to fit observations becomes an important issue.

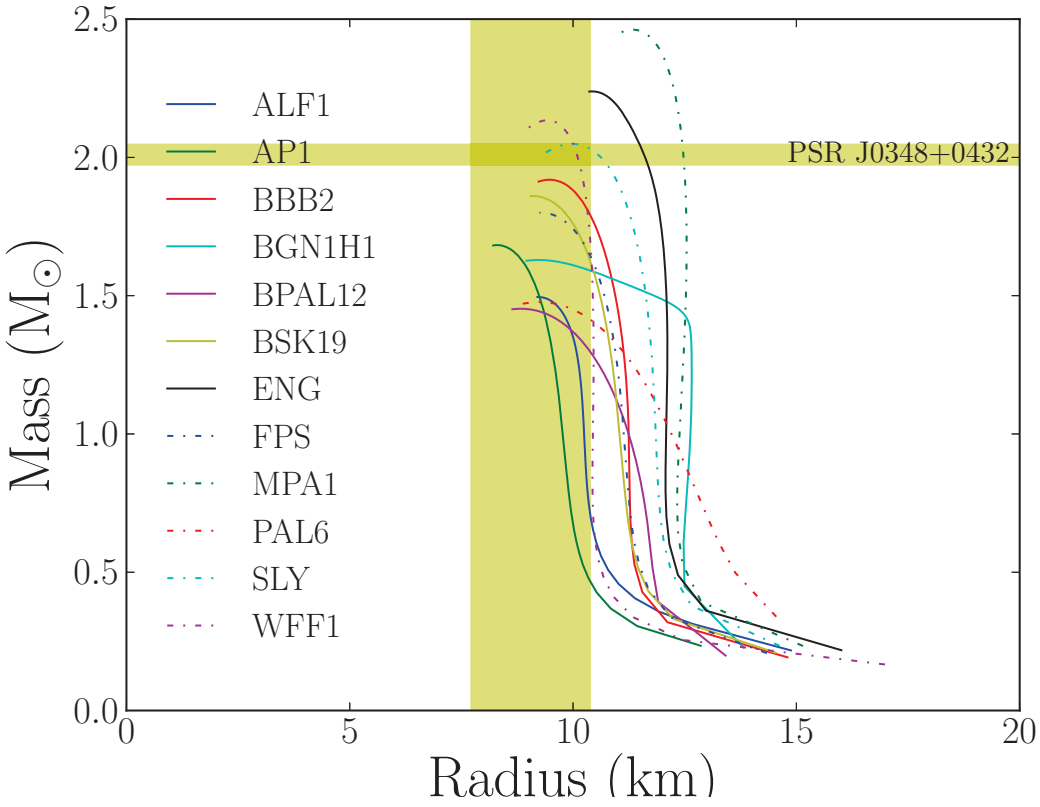

Figure 5.2: M–R relations obtained from the original EOSs. The yellow area shows the 90% confidence constraints on the neutron star radii $R = 9.1^{+1.3}_{-1.5}$ that were proposed by Guillot et al.[18] The mass measurement of PSR J0384+0432 is shown as the horizontal band.[4] Most EOSs are compatible with large radii of $\approx$12 km.

In principle, neutron star with $2.0M_\odot$ can be obtained by using stiffer EOS at high density but it makes the neutron star radiii too large. Therefore, to make

more realistic constraint to EOS not only mass but also radius should be considered. These difficulties have posed many challenges for theoretical physics. To deal with this problem, we put out below scenario (see Fig. 5.3). Step 1: the phenomenological third-order term ϵ_3 that plays a role in controlling neutron star radii is introduced. Step 2: six linear functions with slopes $\nu_{1,\ldots,6}$ which make it possible to vary the stiffness of EOS at high-density regions . We adjust EOS parameters by the following three conditions:

1. EOS supports neutron star with masses larger than $2.0M_{\odot}$.
2. EOS slopes satisfy $0 < \nu_{1,\ldots,6} \leq 1$ (the causality condition).
3. EOS consists with observational data.

$\nu_{1,\ldots,6}$ and ϵ_3 are optimized independently for each theoritical EOSs. In practice, the n parameter is varied over the ranges $2 \leq n \leq 5$ but after calculating we confirm that $n = 2$ is the best value.

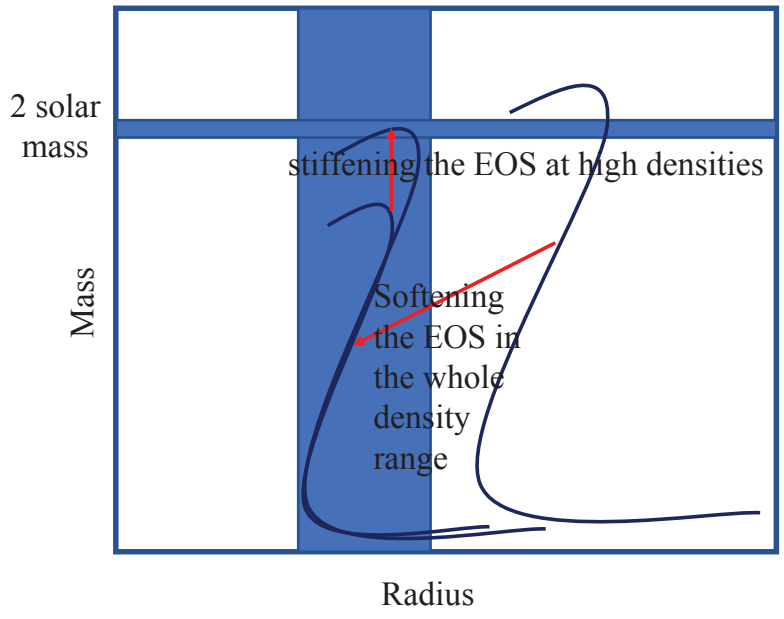

Figure 5.3: Scenario to adjust the EOS to fit the observations. Softening the EOS in the whole density range can produce neutron star with small radii. Stiffening the EOS at high density region is needed to support $2.0M_{\odot}$ neutron star.

Table 5.3 summarize results of the conditional probability $-\log P[\mathcal{M}|D]$ and the EOS parameters. The smaller $-\log P[\mathcal{M}|D]$ corresponds to the better fit, that is, the EOS used is more probable. We can see that for soft EOS models (ALF1, AP1,

WFF1, SLY...) the best fits are obtained with small $\epsilon_3 \approx 0$ and large slopes ν_5, ν_6. This means that we do not need adjust EOS in theoretical region and just stiffen EOS in high-density region. Contrariwise, for stiff EOS models (BGN1H1, ENG, MPA1...) the the best fits are obtained with rather large ϵ_3 and large slopes ν_5, ν_6. It shows that the EOSs at theoretical region need be softened. For both the two trends, we obtain the EOS that is soft in the theoretical region and stiff in the high-density region.

The most probable EOS are shown by silver-shaded region in Fig. 5.4. We find that EOS need to be softened at medium density region (2-4 ρ_0) and have a rapid change of stiffness around $\sim$ 650 MeV/fm^3 energy density ($\sim$3.5 ρ_0). Because the theoretical EOS was not be limited to a specific EOS, conclusions that we obtained here are consistent with our previous results[46] but more general. Our results suggest that some physical mechanisms which lead to a stiffening of EOS would occur around $\sim 3.5\rho_0$ baryon density. At high densities, in general many phase transitions have been considered such as superfluid transitions,[36] kaon or pion condensates,[1,38] hyperon matter,[8] etc. Eventually, phase transitions from nuclear matter to quark matter[14,22] are expected at very high densities. In general, because of the appearance of new degrees of freedom, EOS gets soft after the phase transition. The behavior of our EOS is in contrast to the general phase transitions but is similar to assuming the hadron-quark crossover[27] which leads to a stiffening of EOS. But, we note that our results are obtained based on Bayesian analysis and do not depend on specific physical assumptions about neutron star matter.

For each model of the theoretical EOS, corresponding to the best cases of -log$P[\mathcal{M}|D]$, we draw the M-R relation to compare with probability distributions of observed neutron stars in Figs. 5.5. Neutron star observations used here have small radii $\sim$ 10 km. Our results support that neutron stars with mass 2.0 $M_\odot$ have small radius $\sim$10 km. These M-R curves is consistent with our above remark on the soft theoretical EOS. The EOS which is stiff in both the theoretical and the parameterized EOS regions may not be denied. But this type of EOS cannot give high probability because of large radii and is disfavored by the present 23 observational data used in this work. Indeed, we must emphasize that because of the systematic errors in neutron star radius measurements, this behavior of our EOS must be confirmed in future.

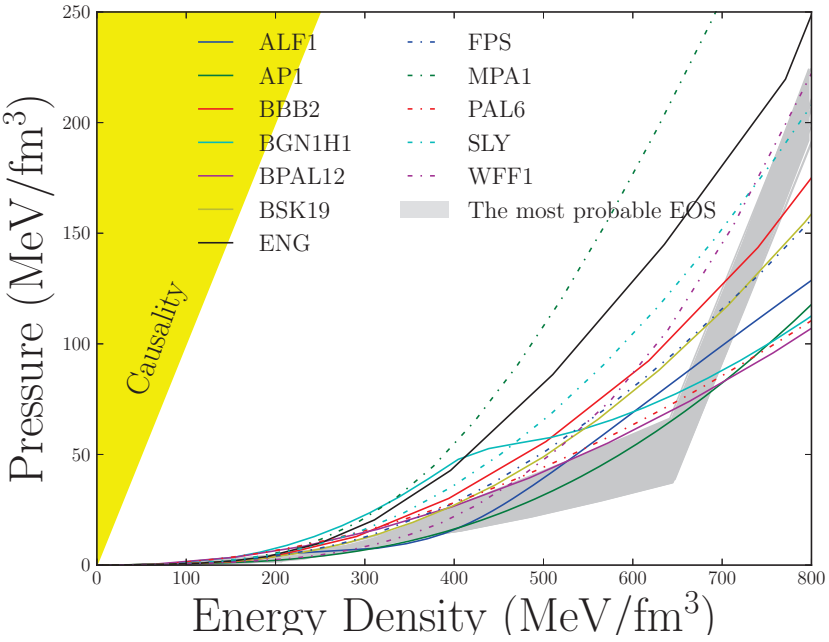

Figure 5.4: Pressure versus energy density for EOS models. The most probable EOSs are shown by the silver-shaded region. Solid lines show the original EOSs. The yellow region shows the causality condition.

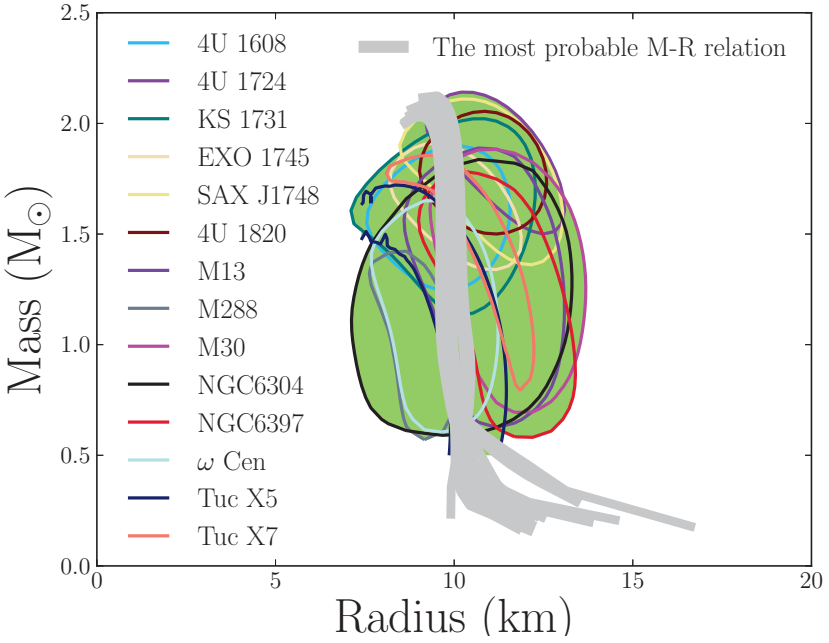

Figure 5.5: Comparison of the probable M–R relations with the observations. The silver band shows the most probable M–R relations implied by observational data.

Model	n	ϵ_3	ν_1	ν_2	ν_3	ν_4	ν_5	ν_6	$-\log P(\mathcal{M}\|D)$
ALF1	2	0.1195	0.0686	0.0853	0.1020	0.1020	0.9990	0.9998	112.2851
AP1	2	0.0546	0.0915	0.0973	0.1630	0.1740	0.9790	0.9973	112.4218
BBB2	2	-0.4415	0.1140	0.1150	0.1170	0.1710	0.9999	0.9999	112.4378
BGN1H1	2	-0.9999	0.1110	0.1110	0.1110	0.2070	0.9430	0.9971	112.6734
BPAL12	2	-0.4280	0.0813	0.0893	0.1301	0.1308	0.9999	0.9999	112.3494
BSK19	2	0.3040	0.0939	0.1001	0.1347	0.1691	0.9870	0.9995	112.3993
ENG	2	-0.7970	0.1320	0.1315	0.1377	0.1470	0.9626	0.9913	112.8413
FPS	2	-0.3063	0.0984	0.0990	0.1110	0.1120	0.9999	0.9999	112.3811
MPA1	2	-0.9999	0.1620	0.1620	0.1620	0.1714	0.9997	0.9999	114.5707
PAL6	2	-0.5381	0.0563	0.0801	0.0932	0.1023	0.9802	0.9985	112.1935
SLY	2	0.1125	0.1130	0.1160	0.1300	0.1393	0.9401	0.9990	112.4660
WFF1	2	-0.0619	0.0994	0.1003	0.1737	0.1745	0.9979	0.9999	112.4280

Table 5.3: Conditional probability $P(\mathcal{M}|D)$. Value of $P(\mathcal{M}|D)$ express possibility of EOS.

5.3 Structure of Neutron Stars

We now enter the study of neutron star structure. The observations of neutron star masses and radii have played an important role in imposing constraints on the EOS of neutron star matter. In section 5.2, we have determined that the EOS needs to be softened in vicinity of the saturation density and to have a rapid change of stiffness around an energy density of 650 MeV/fm^3. In this section, for a given mass, based on this EOS, we study the internal structure of neutron star. Corresponding to three EOS regions, we split the neutron star structure into three main layers: the crust, the outer core and the inner core (see Fig. 5.6). Our aim in this section is to determine the thickness of each layer.

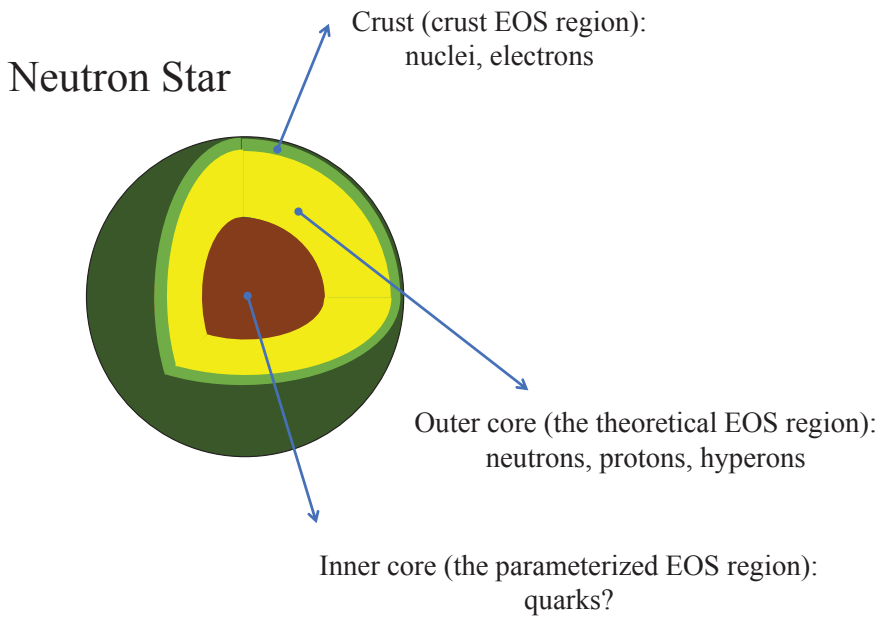

Figure 5.6: Neutron star structure.

We start by analyzing the density profile. In Fig. 5.7, we show calculated profiles of neutron stars with masses M =1.0, 1.4 and 2.0 $M_\odot$. A very interesting point is the radius is independent of mass. For heavy neutron star with mass 2.0 $M_\odot$, we find the small radius ($R < 10$ km) implies very high energy densities in the central region, strongly depending on the EOS in the second region ($\rho_0 < \rho < n\rho_0$). In the case of canonical neutron stars (M = 1.0 and 1.4 $M_\odot$), the central energy density only weakly depends on the EOS in the second region. We have to note that the neutron star radius is primarily determined by the behavior of the theoretical EOS. If we consider rapid change of stiffness is the point marks the beginning of new layer

in the neutron star structure, we can determine the depth of each layer. For 2.0 $M_\odot$ neutron stars, the depth of the crust and the outer core is about 1.5 km. For 1.4 and 1.0 $M_\odot$ neutron stars the depth are 2.5 and 3.5 km respectively. It demonstrates that even though neutron stars have nearly the same radii, there are differences in the depth of each layer depending on mass.

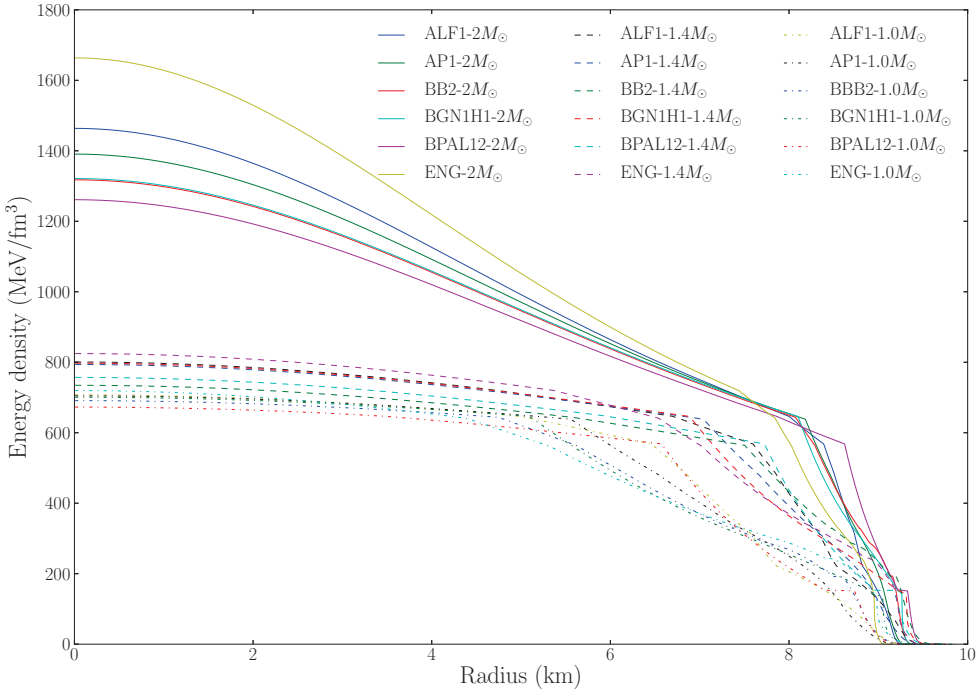

Figure 5.7: Density profiles of 1.0, 1.4, and 2.0 $M_\odot$ neutron stars.

The crust that contains atomic nuclei and free electrons have a thickness of few hundred meters. The outer core layer is composed by baryons. At present, the core region of neutron star is not well known both theoretically and observationally. The composition of the core of the star is particularly uncertain: it may be liquid or solid; it may consist of various hadrons (pions, quarks, hyperons...); and there may be another phase change. Fig. 5.8 illustrates the depth profiles of 1.0, 1.4, and 2.0 $M_\odot$ neutron stars.

Figs. 5.9 and 5.10 show dependence of the mass on central energy density (ε_c) and central pressure (p_c) for some EOSs. On the lower-mass side, the M$-p_c$ and M$-\varepsilon_c$ curves depend rather weakly on the assumed EOS. On the higher-mass side, these curves strongly depends on the assumed EOS. At present, the central energy density and central pressure of a neutron star are unknown but in general, they depend on

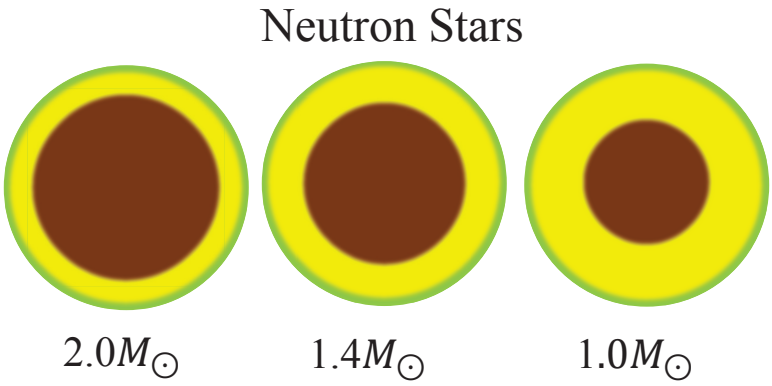

Mass	Crust (volume percent)	Outer core (volume percent)	Inner core (volume percent)
2.0 $M_\odot$	200 m (0.63%)	1.5 km (40.03%)	8.0 km (59.34 %)
1.4 $M_\odot$	200 m (0.63%)	2.5 km (59.62%)	7.0 km (39.75%)
1.0 $M_\odot$	200 m (0.63%)	3.5 km (74.34%)	6.0 km (25.03 %)

Figure 5.8: Neutron star cross section.

mass, the EOS and the composition of the neutron star. However, as a result of this work, for 2.0 $M_\odot$ neutron star, we prospect that the ε_c (p_c) values lie in the region of 1200–1600 (700–1100) MeV/fm^3. A larger mass requires a higher central pressure and hence also higher central energy density to support it. By increasing the central energy and the central pressure, the mass that EOS can support increases but larger pressure means the particles become relativistic. The fact that the mass is getting heavier also means that gravitational attraction becomes stronger and makes the star radius smaller. This means that increasing mass of neutron stars does not make them bigger and makes them denser.

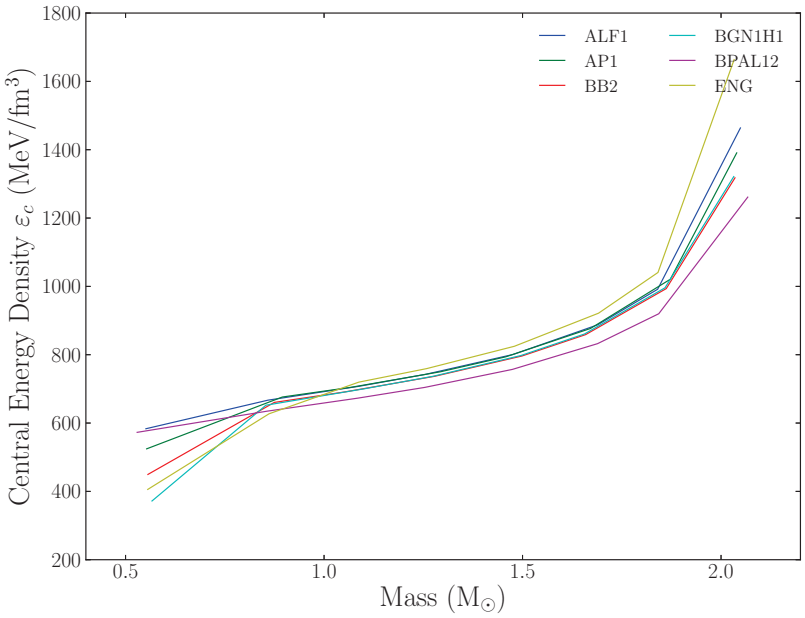

Figure 5.9: Mass versus central energy density for EOS models.

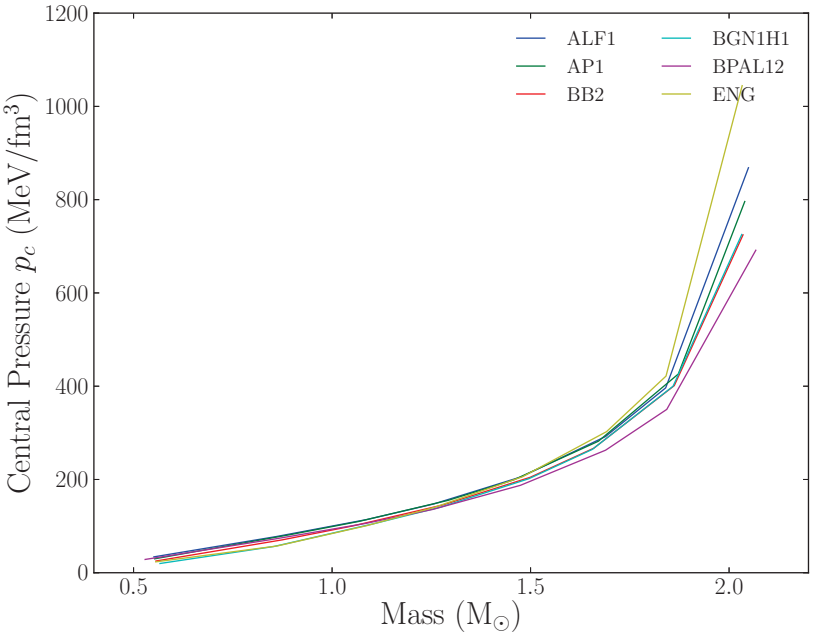

Figure 5.10: Mass versus central pressure for EOS models.

Chapter 6

Summary

The equation of state (EOS) of neutron star matter is a critical subject in nuclear physics research. As of late, neutron star observations have exhibited and started to put essential constraints on the EOS of neutron star matter. We have investigated the EOS of neutron matter using constraints from recent neutron star observations. It is found that the EOS that have the best fit to observations is the EOS softened by the additional third order term of baryon density in the moderate density region (2–$4\rho_0$) and the stiff EOS in the high-density region ($>4\rho_0$). We predict a rapid change of stiffness around 3.5–4.0 times of the saturation density. In addition, for a given mass, based on this EOS, we have studied the internal structure of neutron star. We have demonstrated that the radius depends negligibly on the increasing mass and increasing mass makes the inner stiff core of neutron star bigger. By analyzing 12 EOS models and using a total of 23 probability distributions with improved analyses allow us to place more realistic constraints. More neutron star observations with mass and radius constraints would enable us to improve on results and make calculation more effective.

The enhanced research of the neutron star mass and radius and the laboratory constraints of the properties of dense matter have already had a generous effect on our study of the nuclear matter properties but there are still many challenges in the future. For example, reducing the uncertainties in the neutron star radii and masses, constructing the hot dense matter EOS, demonstrating how to perform the inverse problem: take the M-R relationship, and produce an EOS,[26] etc require further study. But with the appearance of the next generation of X-ray instruments and of advanced gravitational wave detectors, it is optimistic that tighter constraints on neutron star radii will soon be made. Such constraints joined with laboratory measurements will give us essential clues to construct high-density matter EOS.

Appendix A

Physical Constants

Speed of Light	c	=	$2.997\ 924\ 58 \times 10^{8}$ ms^{-1}
Gravitational Constant	G	=	$6.673\ 848 \times 10^{-11}$ m^{3} kg^{-1}s^{-2}
Planck Constant	h	=	$6.626\ 069 \times 10^{-34}$ J s
Reduced Planck Constant	$\hbar = h/2\pi$	=	$1.054\ 571 \times 10^{-34}$ J s
Electron Rest Mass	m_e	=	$9.109\ 382 \times 10^{-31}$ Kg
Elementary Charge	e	=	$1.602\ 177 \times 10^{-19}$ C
Proton Rest Mass	m_p	=	$1.672\ 623 \times 10^{-27}$ Kg
Neutron Rest Mass	m_n	=	$1.674\ 928 \times 10^{-27}$ Kg

Appendix B

Units and Symbols

B.1 Units

MeV	=	1.6022×10^{-6} erg.		
MeV	=	1.7827×10^{-27} g	=	1.1604×10^{10} K.
$\hbar c$	=	197.33 MeV fm.		
e^2	=	1.4400 MeV fm	=	1.3805×10^{-34} cm^2.
fm	=	10^{-13} cm.		
MeV/fm^3	=	1.6022×10^{33} dyne/cm^2.		
1/fm^4	=	197.33 MeV/fm^3.		
1/fm^4	=	3.5178×10^{14} g/cm^3	=	3.1616×10^{35} dyne/cm^2.
$M_\odot$	=	1.989×10^{33} g	=	1.116×10^{60} MeV.

B.2 Symbols

ρ	baryon density	fm^{-3}
ρ_0	saturation density	fm^{-3}
p	pressure	fm^{-4}
ϵ	energy density	fm^{-4}
r	radius	km
M	mass	solar mass
$M_\odot$	solar mass	

Appendix C

Baym-Pethick-Sutherland EOS

ρ (fm^{-3})	ϵ ($\mathrm{g/cm}^3$)	p ($\mathrm{dyne/cm}^2$)	ρ (fm^{-3})	ϵ ($\mathrm{g/cm}^3$)	p ($\mathrm{dyne/cm}^2$)
4.7300E-15	7.8610E+00	1.0100E+09	2.5060E-05	4.1720E+10	4.6280E+28
4.7600E-15	7.9000E+00	1.0100E+10	3.1550E-05	5.2540E+10	5.9490E+28
4.9100E-15	8.1500E+00	1.0100E+11	3.9720E-05	6.6170E+10	8.0890E+28
6.9900E-15	1.1600E+01	1.2100E+12	5.0000E-05	8.3330E+10	1.1000E+29
9.9000E-15	1.6400E+01	1.4000E+13	6.2940E-05	1.0490E+11	1.4950E+29
2.7200E-14	4.5100E+01	1.7000E+14	7.9240E-05	1.3220E+11	2.0330E+29
1.2700E-13	2.1200E+02	5.8200E+15	9.9760E-05	1.6640E+11	2.5970E+29
6.9300E-13	1.1500E+03	1.9000E+17	1.1050E-04	1.8440E+11	2.8920E+29
6.2950E-12	1.0440E+04	9.7440E+18	1.2560E-04	2.0960E+11	3.2900E+29
1.5810E-11	2.6220E+04	4.9680E+19	1.5810E-04	2.6400E+11	4.4730E+29
3.9720E-11	6.5870E+04	2.4310E+20	1.9900E-04	3.3250E+11	5.8160E+29
9.9760E-11	1.6540E+05	1.1510E+21	2.5060E-04	4.1880E+11	7.5380E+29
2.5060E-10	4.1560E+05	5.2660E+21	2.5720E-04	4.2990E+11	7.8050E+29
6.2940E-10	1.0440E+06	2.3180E+22	2.6700E-04	4.4600E+11	7.8900E+29
1.5810E-09	2.6220E+06	9.7550E+22	3.1260E-04	5.2280E+11	8.3520E+29
3.9720E-09	6.5880E+06	3.9110E+23	3.9510E-04	6.6100E+11	9.0980E+29
5.0000E-09	8.2940E+06	5.2590E+23	4.7590E-04	7.9640E+11	9.8310E+29
9.9760E-09	1.6550E+07	1.4350E+24	5.8120E-04	9.7280E+11	1.0830E+30
1.9900E-08	3.3020E+07	3.8330E+24	7.1430E-04	1.1960E+12	1.2180E+30
3.9720E-08	6.5900E+07	1.0060E+25	8.7860E-04	1.4710E+12	1.3000E+30
7.9240E-08	1.3150E+08	2.6040E+25	1.0770E-03	1.8050E+12	1.5000E+30
1.5810E-07	2.6240E+08	6.6760E+25	1.3140E-03	2.2020E+12	1.7000E+30
1.9900E-07	3.3040E+08	8.7380E+25	1.7480E-03	2.9300E+12	1.9000E+30
3.1550E-07	5.2370E+08	1.6290E+26	2.2870E-03	3.8330E+12	2.2000E+30
5.0000E-07	8.3010E+08	3.0290E+26	2.9420E-03	4.9330E+12	2.7000E+30
6.2940E-07	1.0450E+09	4.1290E+26	3.7260E-03	6.2480E+12	3.2000E+30
7.9240E-07	1.3160E+09	5.0360E+26	4.6500E-03	7.8010E+12	3.8000E+30
9.9760E-07	1.6570E+09	6.8600E+26	5.7280E-03	9.6120E+12	4.5000E+30

table continued on next page

continued from previous page

ρ (fm^{-3})	ϵ ($\mathrm{g/cm}^3$)	p ($\mathrm{dyne/cm}^2$)	ρ (fm^{-3})	ϵ ($\mathrm{g/cm}^3$)	p ($\mathrm{dyne/cm}^2$)
1.5810E-06	2.6260E+09	1.2720E+27	7.4240E-03	1.2460E+13	5.4000E+30
2.5060E-06	4.1640E+09	2.3560E+27	8.9070E-03	1.4960E+13	6.4000E+30
3.9720E-06	6.6020E+09	4.3620E+27			
5.0000E-06	8.3130E+09	5.6620E+27			
6.2940E-06	1.0460E+10	7.7020E+27			
7.9240E-06	1.3180E+10	1.0480E+28			
9.9760E-06	1.6590E+10	1.4250E+28			
1.2560E-05	2.0900E+10	1.9380E+28			
1.5810E-05	2.6310E+10	2.5030E+28			
1.9900E-05	3.3130E+10	3.4040E+28			

Table C.1: Equation of state of BPS.[15]

Bibliography

[1] A. Akmal and V. R. Pandharipande. Spin-isospin structure and pion condensation in nucleon matter. *Phys. Rev. C*, 56:2261, 1997.

[2] A. Akmal, V. R. Pandharipande, and D. G. Ravenhall. Equation of state of nucleon matter and neutron star structure. *Phys. Rev. C*, 58:1804, 1998.

[3] M. Alford, M. Braby, M. Paris, and S. Reddy. Hybrid stars that masquerade as neutron stars. *Astrophys. J.*, 629:969, 2005.

[4] J. Antoniadis, P. C. C. Freire, N. Wex, T. M. Tauris, R. S. Lynch, M. H. van Kerkwijk, M. Kramer, C. Bassa, V. S. Dhillon, T. Driebe, J. W. T. Hessels, V. M. Kaspi, V. I. kondratiev, N. Langer, T. R. Marsh, M. A. McLaughlin, T. T. Pennucci, S. M. Ransom, I. H. Stairs, J. van Leeuwen, J. P. W. Verbiest, and D. G. Whelan. A massive pulsar in a compact relativistic binary. *Science*, 340:6131, 2013.

[5] S. Balberg and A. Gal. An effective equation of state for dense matter with strangeness. *Nucl. Phys, A*, 625:435, 1997.

[6] M. Baldo, I. Bombaci, and G. F. Burgio. Microscopic nuclear equation of state with three-body forces and neutron star structure. *Astron. Astrophys. J.*, 328:274, 1997.

[7] Baym, C. Pethick, and P. Sutherland. The ground state of matter at high densities: Equation of state and stellar models. *Astrophysical Journal*, 170:299, 1971.

[8] G. Baym and C. Pethick. Physics of neutron star. *Annual Review of Astronomy and Astrophysics*, 17:415, 1979.

[9] P. B. Demorest, T. Pennucci, S. M. Ransom, M. S. E. Roberts, and J. W. T. Hessels. A two-solar-mass neutron star measured using shapiro delay. *Natural*, 467:1081, 2010.

[10] F. Douchin and P. Haensel. A unified equation of state of dense matter and neutron star structure. *Astron. Astrophys.*, 380:151, 2001.

[11] L. Engvik and E. Osnes. Asymmetric nuclear matter and neutron star properties. *Astrophys. J.*, 469:794, 1996.

[12] B. Friedman and V. R. Pandharipande. Hot and cold, nuclear and neutron matter. *Nucl. Phys, A*, 361:502, 1981.

[13] N. Glendenning and S. Moszkowski. Reconciliation of neutron-star and binding of the gamma in hypernuclei. *Physical Review Letters*, 67:2414–2417, 1991.

[14] N. K. Glendenning. First-order phase transitions with more than one conserved charge: Consequences for neutron stars. *Phys. Rev. D*, 46:1274, 1992.

[15] N. K. Glendenning. *Compact Stars*. Springer, 2000.

[16] N. K. Glendenning and J. Schaffner-Bielich. First order kaon condensate. *Phys. Rev. C*, 60:025803, 1999.

[17] S. Guillot, R. E. Rutledge, and E. F. Brown. Neutron star radius measurement with the quiescent low-mass X-ray binary U24 in NGC 6397. *The Astrophysical Journal*, 732:88, 2011.

[18] S. Guillot, M. Servillat, N. A. Webbb, and R. E. Rutledge. Measurement of the radius of neutron stars with high signal-to-noise quiescent low-mass X-ray binaries in globular clusters. *The Astrophysical Journal*, 772:7, 2013.

[19] T. Güver, F. Özel, A. Carbera-Lavers, and P. Wroblewski. The distance, mass, and radius of the neutron star in 4U 1608-52. *The Astrophysical Journal*, 712:964, 2010.

[20] T. Güver, P. Wroblewski, L. Camarota, and F. Özel. The mass and radius of the neutron star in 4U 1820-30. *The Astrophysical Journal*, 719:1807, 2010.

[21] C. O. Heinke, G. B. Rybicki, R. Narayan, and J. E. Grindlay. A hydrogen atmosphere spectral model applied to the neutron star X7 in the globular cluster 47 Tucanae. *The Astrophysical Journal*, 644:1090, 2006.

[22] H. Heiselberg, C. J. Pethick, and E. F. Staubo. Quark matter droplets in neutron stars. *Phys. Rev. Lett.*, 70:1355, 1993.

[23] T. Katayama, T. Miyatsu, and K. Saito. Equation of state for massive neutron stars. *The Astrophysical Journal Supplement Series*, 203:22, 2012.

[24] B. D. Lackey and M. Nayyar. Observational constraints on hyperons in neutron stars. *Phys. Rev. D*, 73:024021, 2006.

[25] J. M. Lattimer and A. W. Steiner. Constraints on the symmetry energy using the mass-radius relation of neutron stars. *Eur. Phys. J. A*, 50:40, 2014.

[26] L. Lindblom. Determining the nuclear equation of state from neutron-star masses and radii. *The Astrophysical Journal*, 398:569, 1992.

[27] K. Masuda, T. Hatsuda, and T. Takatsuka. Hadron-quark crossover and massive hybrid stars. *Prog. Theor. Exp. Phys.*, 073D01:1, 2013.

[28] T. Miyatsu, S. Yamamuro, and K. Nakazato. A new equation of state for neutron star matter with nuclei in the crust and hyperons in the core. *The Astrophysical Journal*, 777:4, 2013.

[29] H. Müther, M. Prakash, and T. L. Ainsworth. The nuclear symmetry energy in relativistic brueckner-hartree-fock calculations. *Phys. Lett. B*, 199:469, 1987.

[30] H. Müther and B. D. Serot. Relativistic mean-field theory and the high-density nuclear equation of state. *Nucl. Phys, A*, 606:508, 1996.

[31] S. Nishizaki, Y. Yamamoto, and T. Takatsuka. Hyperon-mixed neutron. *Progress of Theoretical Physics*, 108:703, 2002.

[32] J. Oppenheimer and G. Volkoff. On massive neutron cores. *Phys. Rev.*, 55:374, 1939.

[33] F. Özel, A. Gould, and T. Guver. The mass and radius of the neutron star in the bulge low-mass X-ray binary KS 1731-260. *The Astrophysical Journal*, 748:5, 2012.

[34] F. Özel, T. Guver, and D. Psaltis. The mass and radius of the neutron star in EXO 1745-248. *The Astrophysical Journal*, 693:1775, 2009.

[35] F. Özel, D. Psaltis, T. Gver, G. Baym, C. Heinke, and S. Guillot. The dense matter equation of state from neutron star radius and mass measurements. *The Astrophysical Journal*, 820:28, 2016.

[36] D. Page, M. Prakash, J. M. Lattimer, and A. W. Steiner. Rapid cooling of the neutron star in cassiopeia a triggered by neutron superfluidity in dense matter. *Phys. Rev. Lett.*, 106:081101, 2011.

[37] D. Page and S. Reddy. Dense matter in compact stars: Theoretical developments and observational constraints. *Ann. Rev. Nucl. Part. Sci.*, 56:327, 2006.

[38] V. R. Pandharipande, C. J. Pethick, and V. Thorsson. Kaon energies in dense matter. *Phys. Rev. Lett.*, 75:4567, 1995.

[39] A. Potehkin, A. Fantina, N. Chamel, J. Pearson, and S. Goriely. Astructure representations of unified equation of state for neutron-star matter. *A&A*, 560:48, 2013.

[40] M. Prakash, T. L. Ainsworth, and J. M. Lattimer. Equation of state and the maximum mass of neutron stars. *Phys. Rev. Lett.*, 61:2518, 1988.

[41] M. Prakash, J. R. Cooke, and M. L. J. Quark-hadron phase transition in protoneutron stars. *Phys. Rev. D*, 52:661, 1995.

[42] N. K. G. Schaffner-Bielich. First order kaon condensate. *Phys. Rev. C*, 60:025803, 1999.

[43] A. W. Steiner, J. M. Lattimer, and E. F. Brown. The neutron star mass-radius relation and the equation of state of dense matter. *The Astrophysical Journal*, 765:L5, 2013.

[44] A. W. Steiner, J. M.Lattimer, and E. F.Brown. The equation of state from observed masses and radii of neutron star. *The Astrophysical Journal*, 722:33, 2010.

[45] J. R. Stone, P. Guichon, H. Matevosyan, and A. Thomas. Cold uniform matter and neutron stars in the quark-meson-coupling model. *Nuclear Physics A*, 792:341–369, 2007.

[46] N. Q. Thin and S. Shinmura. The equation of state of neutron star matter based on the G-matrix and observations. *Prog. Theor. Exp. Phys.*, 073D02, 2016.

[47] R. C. Tolman. Static solutions of einstein's field equations for spheres of fluid. *Phys. Rev.*, 55:364, 1939.

[48] I. Vidana. Hyperons and neutron stars. *Nuclear Physics A*, 914:367–376, 2013.

[49] N. A. Webbb and D. Barret. Constraining the equation of state of supranuclear dense matter from XMM-NEWTON observations of neutron stars in globular clusters. *The Astrophysical Journal*, 671:727, 2007.

[50] F. Weber, R. Negreiros, P. Rosenfield, and M. Steijner. Pulsar as astrophysical laboratories for nuclear and particle physics. *Prog. Part. Nucl. Phys.*, 59:94, 2007.

[51] S. Weissenborn, D. Chatterjee, and J. Schaffner-Bielich. Hyperons and massive neutron stars: Vector repulsion and SU(3) symmetry. *Phys. Rev. C*, 85:065802, 2012.

[52] R. B. Wiringa, V. Fiks, and A. Fabrocini. Equation of state for dense nucleon matter. *Phys. Rev. C*, 38:1010, 1988.

[53] Y. Yamamoto, T. Furumoto, N. Yasutake, and T. A. Rijken. Multi-pomeron repulsion and the neutron-star mass. *Phys. Rev. C*, 88:022801(R), 2013.

[54] W. Zuo, I. Bombaci, and U. Lombardo. Asymmetric nuclear matter from an extended brueckner-hartree-fock approach. *Phys. Rev. C*, 60:024605, 1999.

List of publications by the author

Journal Publications

1. Ngo Quang Thin and Shoji Shinmura,"The equation of state of neutron star matter based on the G-matrix and observations", Progress of Theoretical and Experimental Physics, Volume 2016, Issue 7, 073D02 (18 pages) (2016).

2. Ngo Quang Thin and Shoji Shinmura, "Constraints on the equation of state of neutron star matter based on observations", Modern Physics Letters A (2017), Volume 32, 1750190 (11 pages) (2017),

Domestic Conference Publications

1. Ngo Quang Thin and Shoji Shinmura "Constraints on neutron-star mass-radius relation by the EOS derived from realistic interactions", The Fourth Joint Meeting of the Nuclear Physics Divisions of the American Physical Society and The Physical Society of Japan Hawaii (2014).

2. Ngo Quang Thin and Shoji Shinmura, "Statistical methods to constraints on the EOS of neutron-star", The Physical Society of Japan Annual Meeting, Tokyo (2015).

3. Ngo Quang Thin and Shoji Shinmura, "Constraints on the EOS of neutron-star based on statistical method", The Physical Society of Japan Autumn Meeting, Osaka (2015).

4. Ngo Quang Thin and Shoji Shinmura, "Constraints on the Neutron Star Matter EOS Based on the Mass-Radius Observations", The Physical Society of Japan Autumn Meeting, Miyazaki (2016).

5. Ngo Quang Thin and Shoji Shinmura, "Constraints on the Neutron Star Matter EOS Based on the Mass-Radius Observations (II)", The Physical Society of Japan Annual Meeting, Osaka (2017).

6. Ngo Quang Thin and Shoji Shinmura, "The Internal Structure of Neutron Stars", The Physical Society of Japan Annual Meeting, Tokyo (2018).